the dimensionless wavenumber σ of the longitudinal vortices becomes smaller. It might be expected from the Görtler's calculation[1] that a too small value of η_m results in an overestimation of the Görtler parameter G in the state of neutral stability. Instead of the outer boundary condition for $\eta \to \infty$, we use the three following identities for the outside of the boundary layer ($\eta \geqq \eta_e$), which are obtained from Eqs. (2) and (3) with $\bar{u}_0 = 1.0$ and $D\bar{u}_0 = 0$

$$D\bar{u}_1 + \lambda_1 \bar{u}_1 = 0 \tag{4}$$

$$D^2\bar{v}_1 + (\lambda_1 + \sigma)D\bar{v}_1 + \sigma\lambda_1\bar{v}_1 = k(\sigma - \lambda_1)\bar{u}_1 \tag{5}$$

$$D^3\bar{v}_1 + (\lambda_1 + \sigma)D^2\bar{v}_1 + \sigma\lambda_1 D\bar{v}_1 = k(\sigma - \lambda_1)D\bar{u}_1 \tag{6}$$

in which

$$\lambda_1 = [(\bar{v}_{0\infty}{}^2 + 4\sigma^2)^{1/2} - \bar{v}_{0\infty}]/2$$

and

$$k = 2\sigma^2 G^2/\{(\lambda_1{}^2 - \sigma^2)(2\lambda_1 + \bar{v}_{0\infty})\}$$

$\bar{v}_{0\infty}$ denotes the value of $\bar{v}_0$ for $\eta \to \infty$.

Results and Discussion

The instability problem is now reduced to find the Görtler parameter G as an eigenvalue together with two components $\bar{u}_1(\eta)$ and $\bar{v}_1(\eta)$ of the perturbation velocities as eigenfunctions. The system of the differential Eqs. (2) and (3) was numerically solved by the method of successive approximation. In Fig. 1 the solid lines show neutral stability curves in relation of the parameter G to the dimensionless wavenumber σ of the longitudinal vortices for several values of the suction parameter C. The stable range is below each neutral stability curve. The curve for $C = 0$ is compared with the previous results in the case without suction (shown as the broken lines *a*, *b*, and *c*). The curve *a* was first calculated by Görtler,[1] the curve *b* by Hämmerlin[2] with higher approximation but with an assumption $v_0 = 0$, and the curve *c* with Galerkin's method by Smith,[4] who considered the streamwise growth of laminar boundary layer. It is found that the boundary layer is less stable when the normal component v_0 is considered. This effect appears to be more remarkable than that[5] for Tollmien-Schlichting instability of a laminar boundary layer along a flat plate. The minimum value of G is found in the case with suction ($C \gtrsim 1.4639$). The value of the Görtler parameter increases as the suction parameter C is increased, and the laminar boundary layer is stabilized. The curve *d* is the neutral curve[6,7] for the so-called asymptotic suction profile $\bar{u}_0 = 1 - \exp(-0.5y/\theta)$. As expected, the present result tends to the curve *d* when $C \to \infty$. Blowing ($C < 0$) gives little effect on the G-value in the state of neutral stability.

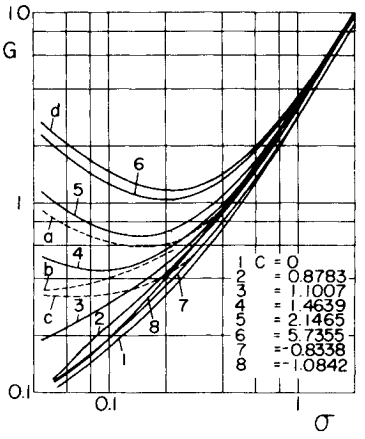

Fig. 1 Neutral stability curves in relation between Görtler parameter G and dimensionless wavenumber σ of longitudinal vortices. Broken lines, in the case without suction, are curve *a*: Görtler,[1] curve *b*: Hämmerlin,[2] and curve *c*: Smith.[4] Solid lines, in the case with suction, are ($C > 0$) or blowing ($C < 0$); curve *d*: Kobayashi[6,7] for asymptotic suction profile.

References

[1] Görtler, H., "Über eine dreidimensionale Instabilität laminarer Grenzschichten an konkaven Wänden," *Nachrichten von der Gesellschaft der Wissenschaften zu Göttingen, mathematisch-physikalische Klasse, neue Folge, Fachgruppe I*, Bd. 2, Nr. 1, 1940, S. 1–26.

[2] Hämmerlin, G., "Über das Eigenwertproblem der dreidimesionalen Instabilität laminarer Grenzschichten an konkaven Wänden," *Journal of Rational Mechanics and Analysis*, Vol. 4, No: 2, March 1955, pp. 279–321.

[3] Schlichting, H., *Boundary Layer Theory*, 4th ed., McGraw-Hill, New York, 1962, p. 276.

[4] Smith, A. M. O., "On the Growth of Taylor-Görtler Vortices along Highly Concave Wall," *Quarterly of Applied Mathematics*, Vol. 13, No. 3, Oct. 1955, pp. 233–262.

[5] Barry, M. D. J. and Ross, M. A. S., "The Flat Plate Boundary Layer. Part 2. The Effect of Increasing Thickness on Stability," *Journal of Fluid Mechanics*, Vol. 43, Pt. 4, 1970, pp. 813–818.

[6] Kobayashi, R., "Note on the Stability of a Boundary Layer on a Concave Wall with Suction," *Journal of Fluid Mechanics*, Vol. 52, Pt. 2, March 1972, pp. 269–272.

[7] Kobayashi, R., "Stability of Laminar Boundary Layer on a Concave Permeable Wall with Homogeneous Suction," *Reports of the Institute of High Speed Mechanics*, Vol. 27, No. 253, March 1973, Tohoku University, Sendai, Japan, pp. 31–47.

Impact of Space Shuttle Orbiter Re-Entry on Mesospheric NO_x

R. S. STOLARSKI,* R. J. CICERONE,† AND A. F. NAGY‡
University of Michigan, Ann Arbor, Mich.

I. Introduction

THEORETICAL modeling of the behavior of minor constituents in the mesosphere is difficult enough even in an assumed steady state but nevertheless, we have performed some time-dependent calculations of odd nitrogen species. The reason we did this was to quantitatively study a situation which has been discussed qualitatively in many circles in the past year or two, namely, what will happen when the proposed space shuttle orbiter re-enters the Earth's atmosphere. The orbiter itself is to be an aircraft 36 m long and 23 m wingspan, weighing 90,000 kg, close to the dimensions of a commercial airliner. Its re-entry is to be characterized by the orbiter's losing most of its orbital kinetic energy along an almost constant altitude leg of its trajectory at about 70 km, extending roughly a quarter of the way round the Earth.

In the shock-heated wake the ambient atmosphere is disturbed; much of the molecular oxygen and nitrogen is converted to nitric oxide, atomic nitrogen, and atomic oxygen. Detailed aerodynamical estimates of the extent of this conversion have been made by Park.[1] Such estimates depend on details of the trajectory, the aircraft materials, and many other aerodynamic considerations. Park has outlined these and shown that for

Presented as Paper 73-525 at the AIAA/AMS International Conference on the Environmental Impact of Aerospace Operations in the High Atmosphere, Denver, Colo., June 11–13, 1973; submitted August 10, 1973; revision received October 12, 1973. This work was supported by NASA Contract NAS 8-23294.

Index categories: Atmospheric, Space, and Oceanographic Sciences; Shock Waves and Detonations.

* Associate Research Physicist, Space Physics Research Laboratory.

† Associate Research Engineer, Space Physics Research Laboratory.

‡ Professor in Electrical Engineering and Atmospheric Sciences.

Table 1 Reactions involving N, NO, and NO^+ below 90 km but above 50 km

1) $h\nu + N_2 \rightarrow N(^4S) + N(^4S)$	J_1
2) $N(^4S) + NO \rightarrow N_2 + O$	2.2×10^{-11}
3) $N(^4S) + O_2 \rightarrow NO + O$	$2.4 \times 10^{-11} \exp(-3975/T)$
4) $N(^4S) + O_2(^1\Delta) \rightarrow NO + O$	3.0×10^{-15}
5) $N(^4S) + O_3 \rightarrow NO + O_2$	$3.0 \times 10^{-11} \exp(-1200/T)$
6) $N(^4S) + O + M \rightarrow NO + M$	$1.0 \times 10^{-32}\, n(M)$
7) $h\nu + NO \rightarrow N(^4S) + O$	J_7
8) $h\nu + NO \rightarrow NO^+ + e$	I_8
9) $NO^+ + e \rightarrow N(^4S) + O$	$2.5 \times 10^{-8}\ (T/1000)^{-1.5}$
10) $NO^+ + e \rightarrow N(^2D) + O$	$7.5 \times 10^{-8}\ (T/1000)^{-1.5}$
11) $N(^2D) + O_2 \rightarrow NO + O$	6.0×10^{-12}
12) $N(^2D) + NO \rightarrow N_2 + O$	2.2×10^{-11}
13) $O_3 + NO \rightarrow NO_2 + O_2$	$9.5 \times 10^{-13} \exp(-1240/T)$
14) $O + NO + M \rightarrow NO_2 + M$	$6.8 \times 10^{-32}\, n(M)$
15) $O + NO \rightarrow NO_2 + h\nu$	6.4×10^{-17}
16) $N(^2D) + O \rightarrow N(^4S) + O$	2.0×10^{-13}
17) $N(^4S) + OH \rightarrow NO + H$	6.8×10^{-11}
18) $NO_2 + O \rightarrow NO + O_2$	$3.2 \times 10^{-11} \exp(-300/T)$
19) $NO_2 + h\nu \rightarrow NO + O$	8.0×10^{-3}
20) $NO_2 + N(^4S) \rightarrow N_2O + O$	1.2×10^{-11}
21) $NO_2 + N(^4S) \rightarrow N_2 + O + O$	1.2×10^{-11}
22) $NO_2 + N(^4S) \rightarrow N_2 + O_2$	1.2×10^{-11}
23) $NO_2 + N(^4S) \rightarrow NO + NO$	0.6×10^{-11}

example one can expect the orbiter to produce an amount of NO of the order of 10% of the orbiter mass on each re-entry. This means about 9000 kg of nitric oxide will be distributed along the re-entry trajectory along a path, say 10^4 km long. Each 1000 kg of NO is about 9×10^{28} molecules so the strength of such a line source is about 10^{21}/cm.

We think it is not too difficult to dismiss the likelihood of global effects of this large local disturbance. One argument proceeds simply by noting that even 100 missions per year adds only 10^6 kg or 1000 tons of NO per year to the mesosphere while natural sources are thought to provide about 100 times more than this. For example, the averaged downward flux of NO from the thermosphere into the mesosphere is of the order of 10^8 kg or 10^5 tons per year if one assumes fluxes like those of Strobel.[2,3]

The more localized disturbance cannot be so easily dismissed. One can note the physical and chemical mechanisms which should act to destroy or dilute the disturbance, namely transport and mixing processes and photochemical reactions. One can also use best guesses of typical wind speeds, molecular and eddy diffusion coefficients, chemical reaction rates and gaseous concentrations and estimate which processes will produce what effects and how fast, and of course, we have done this to get a rough feeling for the duration and extent of the disturbance. But the picture is a complicated one and we wanted to be as quantitative as possible without becoming entangled in the numerical analysis problems so common in modeling. We have thus used a fairly simple model which includes the important photochemistry and transport processes for the mesosphere.

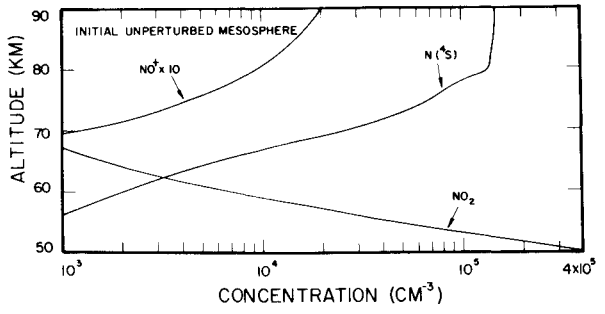

Fig. 1 Undisturbed mesospheric N, NO_2, NO^+ profiles.

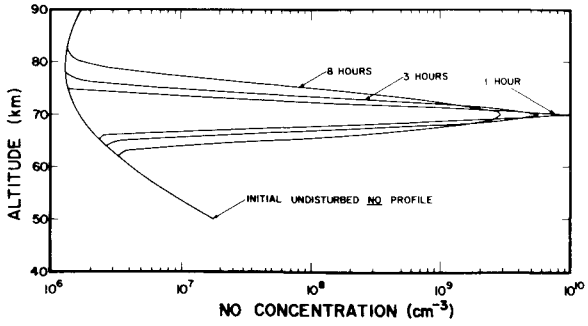

Fig. 2 Undisturbed NO profile with shuttle perturbation for low horizontal diffusion coefficient.

II. Model

Table 1 shows the photochemical reaction scheme. This set of reactions and reaction rates is the same as Strobel's except that we have added several reactions, e.g., $N(^2D) + NO \rightarrow N_2 + O$. By placing our upper boundary at 90 km we can eliminate the need to treat most of the ion-molecule reactions, leaving only (8), (9), and (10) for production and loss of NO^+. The regions above 90 km merely become sources of odd nitrogen for the mesosphere through a downward flux boundary condition; the strength of this source is varied by treating the downward flux as a parameter in the model.

We have used these chemical reactions in a time-dependent continuity equation written for ON ≡ odd nitrogen following Strobel's method. The idea is to lump all the nitrogen constituents except N_2 into one fictitious component called ON then solve the continuity equation for ON, then to use algebra on the resultant profile to solve for all the separate constituent concentrations, like $N(^4S)$, $N(^2D)$, NO, NO_2, and NO^+. This procedure is justified by the fact that chemical lifetimes for these constituents are less than transport times in the mesosphere as Strobel has shown. Thus, the algebraic equations we solve for the separate constituent concentrations are relationships based on photochemical equilibrium. The ON continuity equation itself includes the important transport terms and is written for the range 50 to 90 km.

Figure 1 shows the calculated steady-state mesospheric odd nitrogen densities for the flux boundary conditions; $\phi_{90} = -10^8$, $\phi_{50} = 10^6$ cm^{-2} sec^{-1}. The NO density is off scale and will be seen in a later figure. $N(^2D)$ vanishes on this scale and is not shown. These results indicate one possible natural mesosphere which we have used as the undisturbed mesosphere which is to be perturbed by the shuttle orbiter re-entry.

These profiles are from numerical solutions of a finite-difference form of the one-dimensional continuity equation which includes the chemistry shown in Table 1 and all important transport processes in the vertical. Eddy diffusion is dominant transport term with $K_e = 5 \times 10^4$ at 50 km (as shown by Strobel), 5×10^6 at 90 km, varying exponentially with altitude.

One further feature of the model should be discussed before adding the shuttle orbiter perturbation. Although our model solves a one-dimensional continuity equation in the vertical we also allow for horizontal depletion of the disturbance. This is

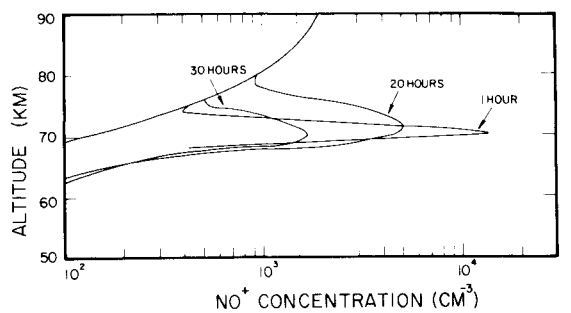

Fig. 3 NO^+ perturbation for low horizontal diffusion coefficient.

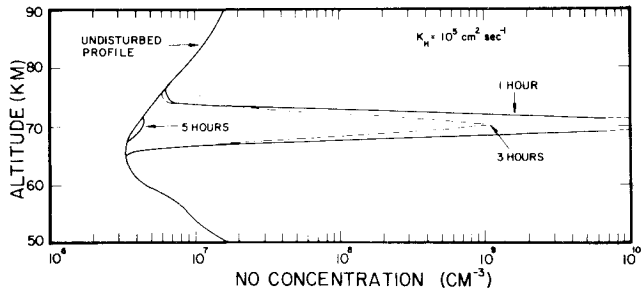

Fig. 4 NO perturbation for horizontal diffusion coefficient = 10^5 cm^2 sec^{-1}.

done by appending to the numerical solution an analytic solution of a diffusion equation in the horizontal. The horizontal eddy or molecular diffusion coefficient appears as a parameter in this diffusion equation. This allows us to watch the material leak out the sides of a box perpendicular to the trajectory of the orbiter. The disturbance has been initially spread into a box 1 km wide in both the horizontal and vertical. That point in time is labeled $t = 0$ and the solution is begun from there considering vertical diffusion plus horizontal depletion from the 1 km box. Thus the perturbed concentrations are averaged over a box (1 km)^2 perpendicular to the trajectory.

Figure 2 shows the undisturbed background profile of NO with several perturbed profiles shown also. The times shown are 1, 3, and 8 hr after the time when the perturbation had spread to $\approx$(1 km)^2 area around the initial wake line source. The horizontal diffusion coefficient was taken to be 10^3 at 50 km up to 10^5 at 90 km varying exponentially. Relaxation to ambient took place after approximately 110 hours. Figure 3 shows NO^+ vs time for the same case. The disturbance is again long lasting and, while easily detectable, is not large in absolute value.

Figures 4 and 5 show similar calculations in which the horizontal diffusion coefficients were taken to be 10^5 cm^2 sec^{-1} independent of altitude. In this case relaxation to ambient took place in $\sim$5 hr. If the horizontal diffusion coefficient is larger yet, there will be a corresponding decrease in the lifetime of the disturbance.

III. Conclusions and Summary

We have modeled the localized effect of a single shuttle orbiter re-entry on mesospheric odd nitrogen. The perturbations of the odd nitrogen species last for a time of the order of hours depending critically upon the value used for the horizontal diffusion coefficient. The processes included in the calculation are the perturbation of NO, photochemical reactions, and horizontal and vertical eddy diffusion. Effects which have not been modeled but may be important are perturbations in N and O, wind shear, diurnal variations, and the influence of heat shield ablation products or water vapor. We have not considered specifically the problem of buildup from repeated orbiter re-entries at the same place. However, the results indicate that even in the worst case the disturbance lifetime is less than 5 days. This combined with the fact that winds will move the disturbance fairly rapidly indicates that there is little possibility of buildup for predicted launch frequencies.

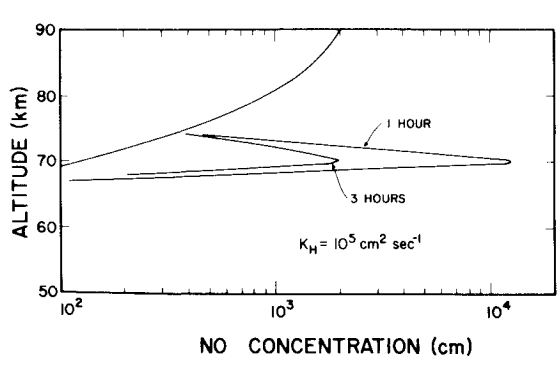

Fig. 5 NO^+ perturbation for horizontal diffusion coefficient = 10^5 cm^2 sec^{-1}.

References

[1] Park, C., "Estimates of Nitric Oxide Production for Lifting Spacecraft Re-entry," Report TM-X-62-052, 1972, NASA.

[2] Strobel, D. F., "Odd Nitrogen in the Mesosphere," *Journal of Geophysical Research*, Vol. 76, 1971b, p. 8384.

[3] Strobel, D. F., "Diurnal Variation of Nitric Oxide in the Upper Atmosphere," *Journal of Geophysical Research*, Vol. 76, 1971, p. 2441.

Correlation of Peak Heating in the Reattachment Region of Separated Flows

RICHARD D. MATTHEWS* AND JEAN J. GINOUX†
von Kármán Institute for Fluid Dynamics, Rhode-Saint-Genèse, Belgium

1. Introduction

VERY high local values of the heat-transfer rate have been measured in the reattachment region of separated boundary layers in high speed flows. Bushnell and Weinstein[1] have derived successful correlation parameters for both laminar and turbulent regimes. The present Note gives some theoretical support to this empirical correlation in the laminar case and shows how the results of some preliminary calculations could lead to a substantial improvement in the correlation technique.

2. Background

The derivation of Bushnell and Weinstein's parameters is based on the assumption that at reattachment a sublayer is formed, the behavior of which is governed by the properties of the incoming boundary layer being compressed above it. The idealized flowfield is shown in Fig. 1.

The authors argue that flat plate-type relationships can be applied in the reattachment region with the peak Stanton number and the corresponding Reynolds number evaluated under local conditions. These correlation parameters are thus defined as the following:

$$(h_{max}/\rho_\omega u_3 c_p)\alpha(\rho_\omega u_3 x_p/\mu_\omega)^{-0.5}$$

where h_{max} = maximum heat-transfer coefficient; ρ_ω = density (note $\rho_\omega \alpha P_3/T_\omega$); μ_ω = viscosity evaluated at wall temperature T_ω; c_p = specific heat at constant pressure; u_3 = inviscid velocity in region 3 (see Fig. 1); and x_p = distance between reattachment and peak heating.

Bushnell and Weinstein are able to correlate the results of six different experiments which involve flap induced laminar boundary-layer separations with freestream Mach numbers

Received August 14, 1973. The calculations were carried out at the von Kármán Institute with partial support of the U.S. Air Force under Grant AFOSR 71-2147.

Index categories: Boundary Layers and Convective Heat Transfer—Laminar; Supersonic and Hypersonic Flow.

* Research Fellow, sponsored by the Royal Society of Great Britain.

† Associate Director; also Professor, Brussels University.